Impact of Persistent Bubbles on Underwater Acoustic Communication

Gabriel Chua
ARL, Tropical Marine Science Institute,
National University of Singapore.

Mandar Chitre
ARL, Tropical Marine Science Institute,
National University of Singapore.

Grant Deane
Scripps Institute of Oceanography,
University of California San Diego.

***Abstract*—Although it is well known that bubbles have a strong influence on underwater acoustic propagation, typical acoustic communication channel models ignore the effect of bubbles. The rationale is that bubbles are only persistently present in the upper water column in special environments such as the surf zone. In other environments, one expects that the bubbles injected by episodic events such as passing ships quickly rise to the surface or dissolve and do not have a long term effect on the communication channel. We believe that bubbles have a large influence on acoustic communications in many environments with seemingly low bubble injection rates, as bubbles affecting typical communication frequency bands can persist in the water for long periods of time. Such environments include waters near shipping lanes, coral reefs, or places with strong winds. In this paper, we present a model for the persistence of bubbles, and validate it with controlled measurements in a wind-wave channel. We show that bubbles affecting medium-range communication systems can persist in the water column for many tens of minutes after they are injected. This can result in a significant impact on underwater acoustic communications.**

I. Introduction

The injection of bubbles by breaking waves, and the evolution of the bubble plumes immediately after the breaking event are well studied. The bubbles within the plume can cause attenuation up to 26 dB/m [1], practically blocking any signal transmission. The Hall-Novarini model [2] has been shown to satisfactorily model acoustic propagation through such bubbly plumes [3], [4]. The model has also been applied in the context of underwater acoustic communication [5], [6]. As reported in [7], these bubbles may not always be bad for acoustic communications, as they may reduce the acoustic interaction with the water surface and create a more benign channel for communications.

Large bubbles injected into the water column rise to the surface due to buoyancy, and typically disappear within a couple of minutes. Therefore acoustic communication channel models often ignore the effect of bubbles. The rationale is that bubbles are only persistently present in the upper water column in special environments such as the surf zone, where breaking waves replenish bubbles regularly. In other environments, one expects that the bubbles injected by episodic events such as a passing ship quickly rise to the surface or dissolve and do not have a long term effect on the communication channel. However, smaller bubbles may stay suspended in the water column due to turbulence [8], until they dissolve and disappear. Studies have shown that the effect of these bubbles can persist for long periods [9], [10]. In this paper, we present a model for the persistence of such bubbles, and validate it with controlled measurements in a wind-wave channel. We show that bubbles affecting medium-range communication systems can persist in the water column for many tens of minutes after they are injected. When injection events occur at similar or shorter intervals (e.g. passing ships, breaking waves, gas release from biological activity, etc), this can result in a significant impact on underwater acoustic communications.

The paper is organized as follows. In section II, we describe the experiment. In section III, we present the results of the experiment. We compare the results with theoretical models in section IV. In section V, we briefly discuss the impact on communication systems. Finally, in section VI, we present our conclusions.

II. The Experiment

A. Experimental setup

The experiment was conducted at the Scripps Institute of Oceanography Wind Wave Channel. We instrumented the channel with an ITC1032 projector to transmit acoustic signals, and two ITC6050C hydrophones as receivers. The schematic of the setup is shown in Fig. 1. We generated waves (about 0.35 m peak-to-peak wave height) using an oscillating paddle. Shortly after that, we turned on the wind (wind speed of 12.6 m/s), and caused the waves to break and inject bubbles. We allowed a stable bubble population to form in the channel over a period of 15 minutes. We then turned off the wind

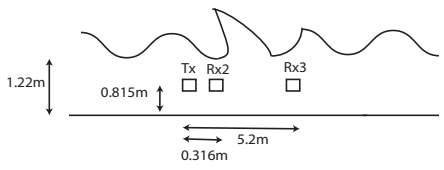

Fig. 1. Schematic of the experimental setup. Tx is the projector used to transmit acoustic signals, and Rx2 is the receiving hydrophone for estimation of bubbles. Rx3 is an additional receiving hydrophone located further in the channel used for reception of m-sequences in section V.

978-1-5386-6442-1/18/$31.00

(waves stopped breaking), but left the waves on, and observed the time evolution of the bubble population.

B. Bubble measurement

We used an acoustic inversion method to obtain bubble population estimates. The projector was used to transmit sinusoidal pulses with frequencies spanning 16.6–85.4 kHz, covering the typical band of interest for medium range acoustic communication. The frequency spacing was optimized based on the method suggested in [11]. This frequency range corresponds to the resonance of 40–190 μm bubbles. A hydrophone was used as a receiver to measure the absorption caused by the bubbles. We measured the absorption, and used the resonance bubble approximation (RBA) in [12] to invert for the bubble size spectral density:

$$n(a) = \frac{\alpha(f) K_r(a,f)}{85.7 a^2} \times 10^{-6}, \tag{1}$$

where,

- $\alpha(f)$ is the absorption in dB/m,
- $K_r(a,f)$ is the real part of the effective wavenumber of the bubbly medium,
- a is the bubble radius in meters,
- $n(a)$, is the bubble spectra density in number of bubbles/m^3/μm.

The absorption $\alpha(f)$ is calculated with [16]:

$$\alpha(f) = \frac{L_{\text{bubbles}}(f) - L_{\text{no bubbles}}(f)}{d}, \tag{2}$$

where, $L_{\text{bubbles}}(f)$ is the transmission loss when bubbles were introduced and $L_{\text{no bubbles}}(f)$ is the transmission loss where there were no bubbles, all losses were measured in dB/m, and d is the distance between the projector and hydrophone. The portion of signal which was included in the calculation of the transmission loss was only from the direct path. Scattering effects from the surface path was intentionally ignored.

Subsequently, the void fraction η is then calculated with [16]:

$$\eta = \frac{4}{3}\pi \int_{a_{\min}}^{a_{\max}} n(a)\, a^3\, da \times 10^6. \tag{3}$$

III. Results

We present results from two datasets. Each dataset was collected for a period of about 45 minutes, and the time between the datasets is 75 minutes.

Fig. 2 shows the void fraction η, as a function of time. In both datasets, we see an initial period with a small η of 10^{-4} or lower (as 10^{-4} is our estimation noise floor due to wave-induced motion of our transducers). Once the wind is started and the waves start breaking, η rapidly increases to 10^{-2} and stabilizes. When the wind is stopped, η starts decaying quickly, primarily from bubble loss due to buoyancy. This decay can be modeled in both datasets as an exponential decay: $\eta(t) = \eta_0^1 e^{-\Gamma_1 t}$, where η_0^1 is the initial void fraction and Γ_1 is the decay rate. After about 5 minutes, the decay rate changes dramatically, signaling a change in regime of bubble loss. We believe that the decay after this time is mostly due to dissolution of the bubbles. In the first dataset, the second region can also be modeled as an exponential decay: $\eta(t) = \eta_0^2 e^{-\Gamma_2 t}$, but with a different decay rate Γ_2. In the second dataset, this region seems almost flat with $\eta = 2 \times 10^{-4}$. However, we are most likely observing a very slow decay, and that the void fraction would return to 10^{-4} or lower after a long time. This can be modeled using the same exponential decay as the first dataset, but with a much slower decay rate. We could not estimate this decay rate because the persistence time was well beyond our data collection period. The reason for the difference in the dissolution rate in the two dataset is discussed in the next section.

Figs. 3 and 4 show the bubble spectra as a function of time. These results support the claim that the initial loss in void fraction is due to loss in large buoyant bubbles, and the bubbles that persist longer are the smaller bubbles.

IV. Discussion

A. Largest suspended bubble size decay

From Figs. 3 and 4, we see that the largest bubbles that stay suspended in the water column are about 140 μm in radius. The rising velocity for such bubbles due to buoyancy is about 2.5 cm/s [13], assuming that they are "dirty" bubbles with some surfactants on them. As long as the downward velocity due to turbulence in the water column exceeds 2.5 cm/s, these bubbles would not be able to escape to the surface. Since we had waves inducing turbulence in the channel, this modest downward velocity of 2.5 cm/s or more is quite reasonable, although we did not explicitly measure it.

Given that the bubbles are trapped under turbulence, the mechanism that determines their persistence is dissolution. Kapodistrias developed a simplified form of the Epstein and Plesset equations that describe the dissolution time of bubbles [14]:

$$1 - \epsilon^2 = \frac{2D}{a_0^2}\frac{C_s}{\rho_a}(1-\gamma)B_t, \tag{4}$$

where $\epsilon = a/a_0$ and $\gamma = C_0/C_s$ is the gas concentration ratio, while B_t is the dissolution time. Using the parameters shown in Table I, an initial bubble size a_0 of 140 μm, and a final bubbles size a of 40 μm (smallest observable bubble size in our experiment), we obtain an estimate of the gas concentration ratio γ to be 0.75. We then numerically solve the differential equation describing the bubble dissolution [15]:

$$\frac{da}{dt} = -D\frac{C_s}{\rho_a}\frac{1-\gamma+\frac{\tau}{\rho_a a}}{1+\frac{2\tau}{3\rho_a a}}[\frac{1}{a}], \tag{5}$$

where $\tau = 2M\sigma/BT$. We used a fourth order Runga-Kutta numerical integration to obtain the curve relating the bubble radius versus time. This curve can be used to estimate the largest bubble size we should observe in the water column, as a function of time. We superimpose this curve on the bubble size spectra measured from the first dataset, in Fig. 3, and show that the dissolution curve fits the decay of the maximum bubble size well from the 20^{th} to the 33^{rd} minute.

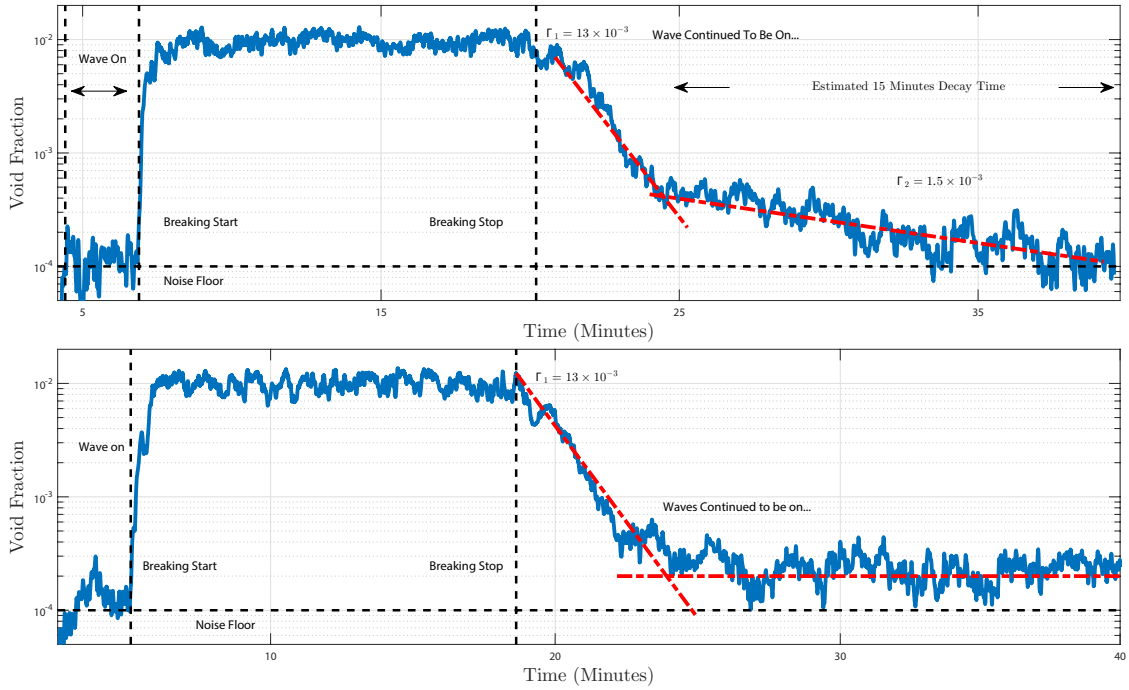

Fig. 2. The upper panel shows void fraction as a function of time from the first dataset, and the lower panel shows void fraction from the second dataset.

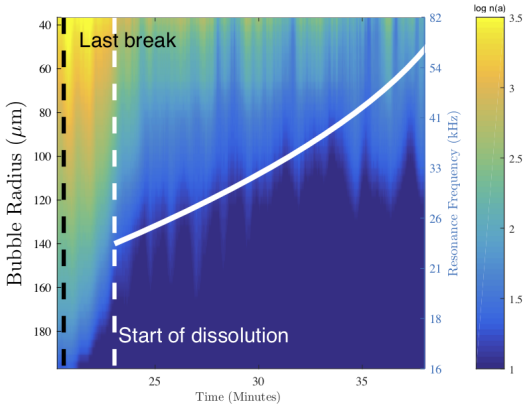

Fig. 3. Bubble spectrum measurement from the first dataset. The white solid line is the dissolution curve from (5), showing the modeled largest bubble size as a function of time.

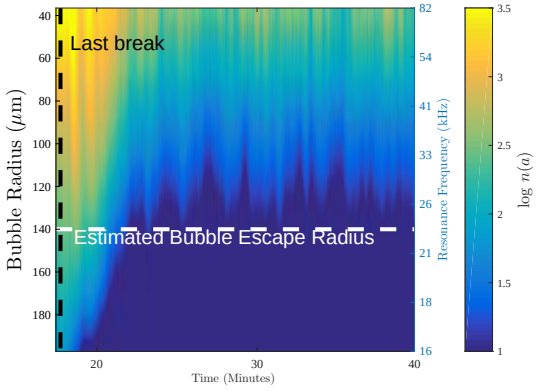

Fig. 4. Bubble spectrum measurement from the second dataset.

After the collection of the first dataset, we expect that the water in the channel had a higher gas concentration ratio than before. Since the second dataset was collected shortly after this, it is reasonable that it started with a higher gas concentration ratio, and therefore has much slower dissolution than in the first dataset. This explains the slower decay of the void fraction and the bubble spectra in the second dataset.

B. Void fraction decay

As seen in Fig 5, the bubble size spectrum at the start of dissolution can be modeled well by a power law:

$$n(a) = n_0 a^{-\nu}, \tag{6}$$

for some constants ν and n_0. We can easily estimate the void fraction for such a bubble size spectrum:

$$\begin{aligned} \eta &= \int_{a_{\min}}^{a_{\max}} n(a)\, \frac{4}{3}\pi a^3\, da \\ &= \frac{4}{3}\pi n_0 \left[\frac{a^{4-\nu}}{4-\nu}\right]_{a_{\min}}^{a_{\max}}, \end{aligned} \tag{7}$$

We know the evolution of $a_{\max}$ from the previous section, and model the decay of the bubbles using $n_0(t) = n_0^0 e^{-bt}$. We

TABLE I
VALUES FOR PARAMETERS IN (4) AND (5) TO OBTAIN THE DISSOLUTION CURVE IN FIG. 3

Symbol	Parameter	Value
D	Diffusivity of water	1.93×10^{-9} m^2/s
a_0	Initial bubble radius	140 μm
a	Final bubble radius	40 μm
C_s	Gas concentration in saturated fresh water	0.024 kg/m^3
ρ_a	Density of air	1.2 kg/m^3
M	Molecular weight of air	0.02897 kg/mol
σ	Surface tension of air	0.0724 N/m
B	Universal gas constant	8.3145 J/(mol K)
T	Temperature	293 K

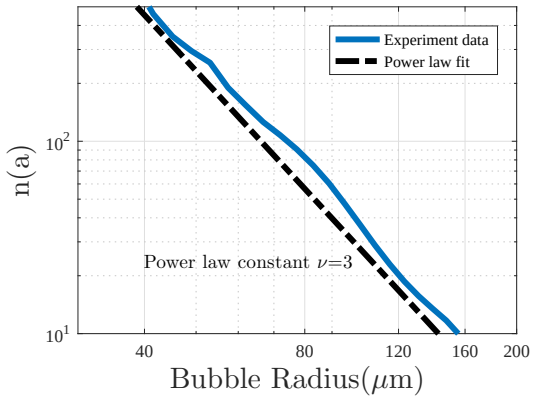

Fig. 5. The bubble spectrum at the start of dissolution is well approximated by a power law.

evaluate the time evolution of the void fraction:

$$\eta(t) = \frac{4}{3}\pi n_0^0 e^{-bt}\left[\frac{a^{4-\nu}}{4-\nu}\right]_{a_{\min}}^{a_{\max}(t)}. \quad (8)$$

using parameters estimated from the data: $a_{min} = 40$ μm, $\nu = 3$, $n_0^0 = 1.2\times10^{-6}$, and $b = 0.0008$. The results are shown in Fig. 6. We see that the model matches the experimental data until the void fraction falls below 10^{-4}, where we are noise limited and unable to accurately measure it.

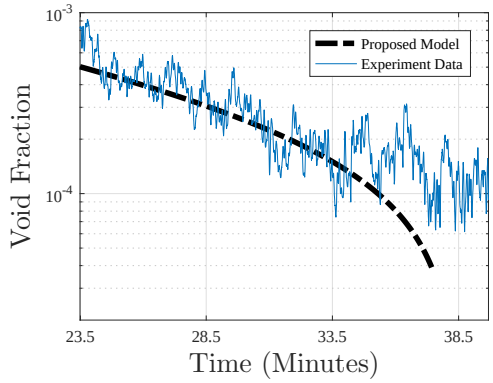

Fig. 6. Modeled v/s measured void fraction from the first dataset.

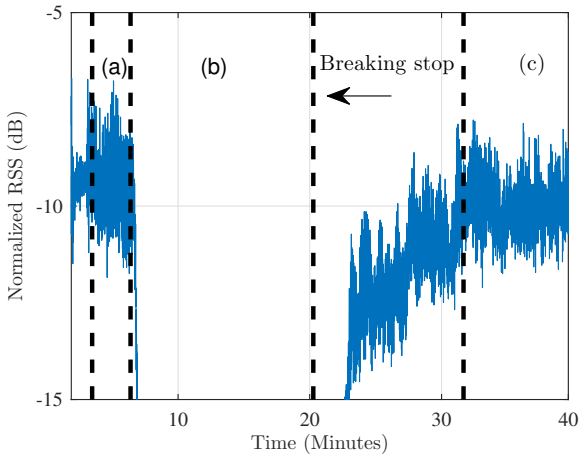

Fig. 7. Received Signal Strength (RSS) of probes sent at Rx3. Period (a) is with waves being generated, (b) with the waves breaking, and (c) with suspended bubbles in the channel, after the waves have stopped breaking for a few minutes. The average RSS during (a) is -9.5 dB, during (b) is about -40 dB (and therefore not shown in the plot), and during (c) is -10 dB.

V. IMPACT ON COMMUNICATION SYSTEMS

In order to study the impact of the bubbles on communication signals, we sent communication probe signals between the projector and the farther receiver (Rx3 in Fig. 1, at a range of 5.2 m) during the experiment. The probes were in the frequency range of 18 kHz to 30 kHz, modulated at baseband data-rate of 12 kbps with a BPSK modulation scheme. We show the received signal strength (RSS) of the probes in Fig. 7. We observe that the RSSI is about -9.5 dB until the waves start breaking, and suddenly drops to about -40 dB once the channel is full of bubbles. After the waves stop breaking, the RSS recovers to about -10 dB and stabilizes. While a 0.5 dB reduction in RSS may not seem much, it is over a short distance of about 5 m. For a typical communication channel of a few hundred meters to a few kilometers, this value would scale up. Imagine a channel with continuous replenishment of bubbles, such a busy shipping lane or a fully developed storm, if the replenishment rate is higher than its decay rate then the effects could be virtually permanent.

VI. CONCLUSIONS

Small bubbles, with resonance frequencies in typical communication band, can persist for long periods of time in the water after a bubble injection event. The persistence is mediated by turbulent forces from waves and currents, and dissolution rates controlled by surfactants and gas concentration in the water. The dynamics of these bubbles can be modeled well using known physics. Such persistent bubbles can have a large and long term impact on communication links, and so modeling them accurately is of great importance.

ACKNOWLEDGEMENT

This work was supported, in part, by ONR Grant N00014-17-1-2633.

REFERENCES

[1] D. M. Farmer, G. B. Deane and S. Vagle, "The influence of bubble clouds on acoustic propagation in the surf zone," IEEE J. Ocean. Eng., Vol. 23 No. 4 pp. 423, Jan 1998.

[2] J. C. Novarini, R. S. keiffer and G. V. Norton, "A model for variations in the range and depth dependence of the sound speed and attenuation induced by bubble clouds under wind-driven sea surfaces," IEEE J. Ocean. Eng., Vol. 23 No. 4 pp. 423, 1998.

[3] R. Vossen and M. Ainslie, "The effect of wind-generated bubbles on sea-surface backscattering at 940 Hz," J. Acoust. Soc. Amer., Vol. 130 Issue: 5 Pp. 3413, 2011.

[4] M. Ainslie, "Effect of wind-generated bubbles on fixed range acoustic attenuation in shallow water at 1-4 kHz," J. Acoust. Soc. Amer., Vol. 118 Issue: 6 Pp. 3513-3523, 2005.

[5] C. A. Boyles, A. P. Rosenberg and Q. Zhang, "Modeling the Effect of Bubble Plumes on High Frequency Acoustic Propagation in Shallow Water," IEEE/MTS 2013 OCEANS - San Diego, 2013.

[6] H. S. Dol, M. Colin, M. Ainslie, P. A. Walree and J. Janmaat, "Simulation of an Underwater Acoustic Communication Channel Characterized by Wind-Generated Surface Waves and Bubbles," IEEE J. Ocean. Eng., Vol. 38, No. 4, Oct. 2013.

[7] P. Walree, "Propagation and Scattering Effects in Underwater Acoustic Communication Channels," IEEE J. Ocean. Eng., Vol 38. No. 4, Oct 2013.

[8] G.B. Deane, J. Preisig and A. Lavery, "The Suspension of Large Bubbles Near the Sea Surface by Turbulence and Their Role in Absorbing Forward-Scattered Sound," IEEE J. Ocean. Eng., Vol 38, No. 4, Pp 632-641 Oct 2013.

[9] Peter H. Dahl, Jee Woong Choi, Neil J. Williams, Hans C. Graber, "Field measurements and modeling of attenuation from near-surface bubbles for frequencies 1-20 kHz.," J. Acoust. Soc. Amer., Vol. 124(3) 2008.

[10] P. H. Dahl, W. J. Plant, B. Nutzel, A. Schmidt, H. Herwig and E. A. Terray, "Simultaneous acoustic and microwave backscattering from the sea surface," J. Acoust. Soc. Amer., Vol. 101(5) page 2583, 1997.

[11] H. Czerski, "An inversion of acoustical attenuation measurements to deduce bubble populations," Journal of Atmospheric and Oceanic Technology 2012.

[12] C.S. Clay and H. Medwin, "Acoustical Oceanography," John Wiley and Sons, pp. 206, 1977.

[13] S. A. Thorpe, "On the Clouds of Bubbles Formed by Breaking Wind-Waves in Deep Water, and their Role in Air Sea Gas Transfer" Philosophical Transactions of the Royal Society of London. Series A Mathematical and Physical Sciences Vol 304, No 1483 1982.

[14] Kapodistrias George, and Peter H. Dahl, "Scattering measurements from a dissolving bubble," J. Acoust. Soc. Amer., Vol 131(6), Pp 4243-4251, 2012.

[15] P. S. Epstein and M. S. Plesset "On the stability of gas bubbles in liquid-gas solutions," J. Chem. Physics 18, 1505–1509 (1950).

[16] S. Stanic, J. Caruthers, R. R. Goodman, E. Kennedy, and R. A. Brown, "Attenuation Measurements Across Surface-Ship Wakes and Computed Bubble Distributions and Void Fractions," IEEE J. Ocean. Eng., Vol 34. No. 1, Jan 2009.